ORIGINAL RESEARCH

Mesenchymal Stem Cell-Derived Exosomes Induced by IL-1β Attenuate Urethral Stricture Through Let-7c/PAK1/NF-κB-Regulated Macrophage M2 Polarization

Ye-Hui Chen[1],*
Ru-Nan Dong[1],*
Jian Hou[1],*
Ting-Ting Lin[1],*
Shao-Hao Chen[1]
Hang Chen[1]
Jun-Ming Zhu[1]
Jia-Yin Chen[1]
Zhi-Bin Ke[1]
Fei Lin[1]
Xue-Yi Xue [1]
Yong Wei [1]
Ning Xu [1,2]

[1]Department of Urology, Urology Research Institute, the First Affiliated Hospital, Fujian Medical University, Fuzhou, 350005, People's Republic of China; [2]Fujian Key Laboratory of Precision Medicine for Cancer, the First Affiliated Hospital, Fujian Medical University, Fuzhou, 350005, People's Republic of China

*These authors contributed equally to this work

Correspondence: Ning Xu; Yong Wei
Department of Urology, Urology Research Institute, the First Affiliated Hospital, Fujian Medical University, 20 Chazhong Road, Fuzhou, 350005, People's Republic of China
Tel +86-059187981687
Email drxun@fjmu.edu.cn; weiyong2017@fjmu.edu.cn

Background: Urethral stricture is a clinical challenge for both patients and clinicians. Post-traumatic urethral stricture is associated with formation of scar tissue caused by excessive inflammation. The aim of this study is exploring potential therapeutic strategies for this condition.

Methods: In vivo experiments on New Zealand rabbits and in vitro experiments on THP-1 monocytes and urethral fibroblasts were performed to investigate the effects on post-traumatic urethral stricture of exosomes isolated from IL-1β-treated mesenchymal stem cells (Exo-MSCs$^{IL-1\beta}$) and the role of macrophage M2 polarization in this process. Additionally, related signaling and mechanism behind were explored.

Results: In a New Zealand rabbit model of post-traumatic urethral stricture, injection of Exo-MSCs$^{IL-1\beta}$ significantly reduced urethral stricture and collagen fiber accumulation compared with Exo-MSCs. Addition of Exo-MSCs$^{IL-1\beta}$ to THP-1 monocytes in vitro induced M2 macrophage polarization, which, in turn, inhibited activation of urethral fibroblasts and synthesis of collagen. Mechanistically, Exo-MSCs$^{IL-1\beta}$ were found to contain high levels of the microRNA let-7c, and luciferase reporter assays showed that let-7c interacted with the 3′UTR of PAK1 mRNA. Transfection of THP-1 cells with a let-7c mimic down-regulated PAK1 expression and inhibited activation of the NF-κB signaling pathway.

Conclusion: These results support a role for let-7c-containing Exo-MSCs$^{IL-1\beta}$ in reducing urethral stricture via inhibition of PAK1–NF-κB signaling, M2 macrophage polarization, and differentiation of urethral myofibroblasts.

Keywords: urethral stricture, mesenchymal stem cells, polarization of macrophages, exosomes, let-7c

Introduction

Urethral stricture is narrowing of the urethral lumen due to fibrosis and scar formation in the urethral mucosa and surrounding tissues.[1–3] Several factors have been implicated in the etiology of this condition, including infection, trauma due to urethral instrumentation, and inflammatory disorders.[4] In each case, urethral epithelial injury heals by fibrosis, resulting in a reduction in urethral diameter and impairment of urine flow.[3,5] Various surgical procedures, such as urethral dilation, urethroplasty, and internal urethrotomy, are available for the treatment of urethral stricture but they have a high failure rate and stricture often recurs.[6–8] Recently

introduced treatments include antifibrotic drugs such as mitomycin C, somatostatin analogs, glucocorticoids, bitoxin A, and halofuginone; however, they have shown little benefit.[9–12] Therefore, there exists an urgent medical need for new strategies for the treatment of urethral stricture.

The process of wound healing after urethral trauma occurs in three overlapping phases: inflammation, proliferation, and remodeling.[13,14] Of these, the inflammation phase is the most appropriate intervention phase to prevent urethral stricture, because hypertrophic repair and scar formation at the wound caused by post-traumatic inflammation are the central processes in urethral stricture.[15,16] Among the many cell types involved in this process, fibroblasts and macrophages play the most important roles as mediators and regulators, respectively, of scar formation and/or degradation.[17] It is well-established that the phenotype of tissue macrophages evolves during wound healing, and also that the macrophage polarization status influences the activation and biological behavior of fibroblasts.[14,18] Pro-inflammatory macrophages, traditionally referred to as M1 macrophages, have positive effects by infiltrating the site of tissue injury or infection and clearing debris, dead cells, and bacteria in the wound. However, excessive inflammation and prolonged activation of fibroblasts can result in scar formation, the ultimate cause of urethral stricture.[19] Ueshima et al also reported that macrophage-secreted TGF-β1 would contribute to fibroblast activation and ureteral stricture after ablation injury.[20] In contrast, M2 macrophages inhibit excessive inflammation and promote wound healing by remodeling of the extracellular matrix.[18] These observations prompted us to consider that enforced macrophage polarization to the M2 subtype could be a potential therapeutic strategy to reduce post-traumatic urethral inflammation and scar formation.

Recent studies have suggested that mesenchymal stem cells (MSCs) can contribute to the resolution of inflammation and facilitate the repair of injured tissues by regulating immune cells in the post-traumatic microenvironment.[21,22] For example, Zhao et al reported that the microRNA (miRNA) miR-182 is present in extracellular vesicles, or exosomes, secreted by MSCs and can attenuate myocardial ischemia–reperfusion injury by regulating macrophage polarization.[23] Additionally, apoptotic bodies derived from MSCs can promote cutaneous wound healing by regulating macrophage function.[24] Inflammatory mediators can induce movement of MSCs to the site of inflammation, where they

alter their secretory profile, exert immunomodulatory effects, and promote wound healing.[25] These observations suggest that cytokines and/or drugs could be used to augment the immunomodulatory characteristics of MSCs and enhance their roles in tissue repair, thus providing a rationale for the development of such treatments for inflammation-related disorders, including urethral stricture.

Pretreatment of MSCs with IL-1β, a key inflammatory mediator, has been reported to enhance the inhibitory effects of MSCs on sepsis-associated systemic inflammation by inducing macrophage polarization towards the anti-inflammatory M2 phenotype.[26] Thus, we hypothesized that IL-1β-induced MSCs may similarly suppress post-traumatic urethral inflammation and scar formation by regulating macrophage polarization. Secretion of exosomes containing various nucleic acids is now recognized as a major mechanism for intercellular communication.[27] Therefore, we speculated that MSCs and macrophages may communicate during urethral wound healing via exosomes. In the present study, we investigated the effects of exosomes derived from IL-1β-induced MSCs on macrophage polarization and fibroblast activation in vitro, and additionally on post-traumatic urethral stricture and fibroblast activation in an animal model. We also explored the underlying mechanism driving the direct effects of Exo-MSCs$^{IL-1\beta}$ on macrophages. The results of our study suggest that miRNA-containing MSC-derived exosomes may be a promising new therapeutic strategy for urethral stricture.

Materials and Methods
Cell Lines and Cell Culture

Specimens of urethral scar tissues were obtained from three patients who underwent urethroplasty for post-traumatic urethral stricture. Primary urethral fibroblasts (UFBs) were obtained and cultured as previously described.[2,3] All experiments with primary cells were performed with the consent of the donors and were approved by the Ethics Committee of the First Affiliated Hospital of Fujian Medical University. Umbilical cord-derived MSCs were purchased from Saliai Stem Cell Science and Technology (Guangzhou, China) and maintained in F12/Dulbecco's modified Eagle's medium (DMEM, Thermo Fisher Scientific Life Sciences, Waltham, MA, USA) containing 10% fetal bovine serum (FBS, Thermo Fisher Scientific Life Sciences). The human monocytic cell-line THP-1 was purchased from the American Type Culture

Collection (Manassas, VA, USA), and was cultured in RPMI medium containing 10% FBS. To induce differentiation into macrophages, THP-1 monocytes were incubated with 100 ng/mL phorbol 12-myristate 13-acetate (PMA, Sigma, St. Louis, MO, USA) for 48 h. For polarization, THP-1 cells were incubated with PMA for 48 h in the presence of 20 ng/mL IL-4 (M2 polarization) or 20 ng/mL IFN-γ and 10 pg/mL lipopolysaccharide (M1 polarization). Transforming growth factor-β1 (TGF-β1) was added at 20 ng/mL to activate UFBs as indicated. All cells were cultured at 37°C in a 5% CO_2 atmosphere.

Isolation and Characterization of Exosomes

MSCs were incubated with or without IL-1β at 50 ng/mL for 48 h. Exosomes were isolated from the culture supernatants by differential centrifugation as previously described, and then characterized using a range of analytical techniques.[28] Exosome morphology was examined by transmission electron microscopy (JEM-200CX, Hitachi, Tokyo, Japan), and size distribution was measured using a NanoSight NS300 system (Malvern Panalytical, Malvern, UK) after dilution of 10 μL isolated exosomes to 1 mL with filtered PBS. The identity of exosomes was confirmed by Western blotting (WB) with antibodies against the exosome marker proteins CD63 and TSG101. Exosomes were quantified by BCA assay of total protein content (Thermo Fisher Scientific Life Sciences). Exosomes from control and IL-1β-primed MSCs were designated Exo-MSCs and Exo-MSCs$^{IL-1\beta}$, respectively.

Animal Model and Urethrography

All animal experiments were approved by the Experimental Animal Ethics Committee of Fujian Medical University, which conformed to the principles of animal protection, animal welfare and ethics, and the relevant provisions of national experimental animal welfare ethics. Twenty-four healthy New Zealand white male rabbits (2.5–3.5 kg) were obtained from the Laboratory Animal Center of Fujian Medical University. Animals were housed in a temperature-controlled (22±1°C), humidity-controlled, (40–70%), and light-period controlled (12 h/12 h light/dark cycle) environment. They were fed a standard rabbit pellet diet and had access to tap water ad libitum. Six animals were randomly selected as the negative control group and received an injection of 100 μL saline into the urethral wall. The remaining animals were

injected in the spongiosum urethra with 1 mg of TGF-β1 in 100 μL of saline to enhance fibrosis and induce the stricture phenotype. All rabbits underwent a partial incision of 1 cm length in the mucosa on the ventral side urethra of the penis using a surgical blade, with an intravenous anesthesia of sodium pentobarbital (30–40 mg/kg). The penile skin wound was subsequently closed using 5–0 absorbable sutures and the urethral catheter then removed. Meloxicam subcutaneously (4 mg/kg) was used for pain relief postoperatively. Two days later, these animals received a second injection into the urethral wall. Six animals in the negative control group received a urethral injection of 100 μL of PBS. The 18 TGF-β1-injected animals were randomly divided into three groups of six rabbits each and received urethral injections of: group 1 (positive control), 100 μL of PBS; group 2, 100 μL of saline containing 30 μg of Exo-MSCs; and group 3, 100 μL of saline containing 30 μg of Exo-MSCs$^{IL-1\beta}$. All injections were performed at the 3, 6, 9, and 12-o'clock positions of the spongiosum urethra percutaneously, where close to the area of incision. Six weeks after surgery, all rabbits underwent retrograde urethrography. An 8F catheter was placed in the urethral orifice and X-ray images were obtained after iodine contrast was injected into the urethra. The urethra diameter was measured for three times at the strictest point, and then the mean was taken. The animals were then immediately euthanized, and the urethral scar tissues were subsequently harvested for histological analysis (Figure 1A).

Western Blotting

Total protein extracts from tissues and cells were prepared using RIPA lysis buffer (Beyotime, Haimen, China) supplemented with PMSF (Beyotime). Sample protein concentration was measured using the bicinchoninic acid kit (Beyotime). Proteins were separated on 8–12% polyacrylamide gels by electrophoresis and subsequently transferred onto polyvinylidene difluoride membranes (Merck Millipore, Darmstadt, Germany). The membranes were blocked with 5% nonfat milk for 1 hour at room temperature and then incubated with primary antibodies overnight at 4°C. After washing with Tris-buffered saline/0.1% Tween 20 (TBST), the membranes were incubated with secondary for 2 hours at room temperature and immunoreactive bands then detected using an enhanced chemiluminescence reagent. Antibodies against TGS101 (ab125011), CD206 (ab64693), iNOS (ab178945) α-SMA (ab240678), PAK1 (ab223849), collagen I (ab34710),
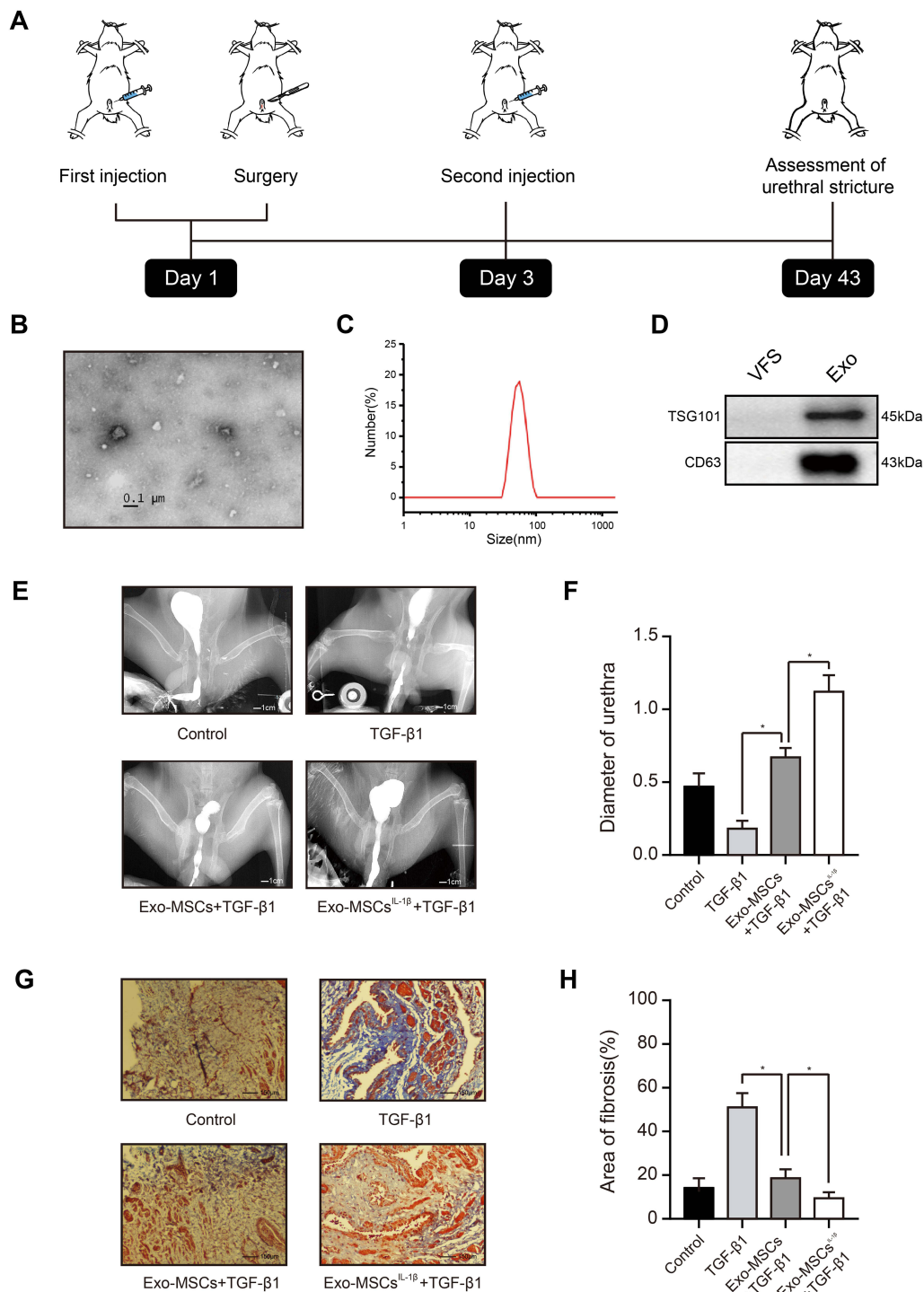
Figure 1 Exosomes from IL-1β-induced MSCs reduce urethral stricture in rabbits. (**A**) Schematic showing the design of animal experiments. (**B**) Transmission electron micrograph of vesicles isolated from MSCs (phosphotungstic acid negative staining). (**C**) Particle diameter distribution from nanoparticle tracking analysis of vesicles isolated from MSCs. (**D**) Western blot analysis of the exosomal markers TSG101 and CD63 in vehicles isolated from MSCs and vesicle-free supernatant. (**E**) Typical retrograde urethrography images of rabbits treated with saline (control), TGF-β1 alone, TGF-β1 + Exo-MSCs, or TGF-β1 + Exo-MSCs$^{IL-1β}$. (**F**) Diameters of urethras from rabbits treated as described for (**E**). (**G**) Representative images of Masson staining of collagen fibrosis in urethral tissue sections from rabbits treated as described for (**E**). (**H**) Quantification of fibrotic area of urethral tissue from rabbits treated as described for (**E**). Data in (**F** and **G**) are presented as the mean ± SD of n = 6 rabbits/group. Statistical analyses were performed with a *t*-test or *t*-test with Welch's correction (**P* < 0.05).
Abbreviations: MSCs, mesenchymal stem cells; Exo-MSCs, exosomes from control MSCs; Exo-MSCs$^{IL-1β}$, exosomes from IL-1β-primed MSCs; VFS, vesicle-free supernatant; TGF-β1, transforming growth factor-β1; α-SMA, α-smooth muscle actin.

collagen III (ab184993), p-p65 (ab31624), p65 (ab32536), p-IKKβ (ab114243), and p-IκBα (ab133462) were obtained from Abcam (Cambridge, MA, USA).

Quantitative Real-Time Polymerase Chain Reaction (qRT-PCR)

Total RNA was extracted using TRIzol reagent (Invitrogen, Carlsbad, CA, USA) according to the manufacturer's instructions. Complementary DNA was synthesized using the PrimeScript RT reagent kit (Takara, Osaka, Japan). qRT-PCR was performed using the SYBR Green assay (Takara) and an ABI 7500 Real-Time PCR System (Applied Biosystems, Waltham, USA).

Masson Staining

Masson staining was used to detect urethral scar fibrosis. The deparaffinized and rehydrated slides were incubated with a Masson staining mixture for 5 min and then stained with a phosphomolybdic acid-aniline blue solution for 6 min. The area of blue-stained collagen fibers relative to the total field of view was calculated using Image-Pro Plus 6.0 software (Media Cybernetics, Rockville, MD, USA).

Transwell Co-Culture System

Transwell co-culture assays were performed using 24-well Transwell plates with 0.4-μm pore diameter inserts (Corning Costar, Corning, NY, USA). THP-1 cells and UFBs were seeded at 5×10^3 cells/well into the upper and lower chambers, respectively (Figure 2C). In this co-culture system, secreted molecules can freely diffuse through the semipermeable membrane while direct contact between the cells is prevented, and cell types can be rapidly separated at the end of the incubation for analysis.

Exosome Labeling and Tracing

Purified exosomes were labeled by incubation with the membrane-labeling dye PKH-67 (Sigma) according to the manufacturer's instructions. Samples were centrifuged at 12,000 ×g for 30 min, excess dye was removed, and unbound dye was neutralized by addition of serum. THP-1 cells were placed in Transwell chambers and treated with 100 ng/mL PMA for 48 h. After being incubated with PKH-67-labeled exosomes (10 μg/mL) for 12 h, washed three times with PBS, they were then incubated with Hoechst 33342 (Sigma) to label nuclei. Images were acquired using an Axiovert A1 microscope (Zeiss GmbH, Jena, Germany).

Immunofluorescence Microscopy

Immunofluorescence microscopy was performed as previously described using an anti-α-SMA primary antibody (1:1000, Abcam) and Ce6-conjugated secondary antibody.[15] After staining, the cells were washed three times with PBS and then fixed with 4% paraformaldehyde for 20 min. The cells were imaged using an A1R-AI confocal microscope (Nikon, Tokyo, Japan) using laser excitation of 543 nm for the detection of Ce6 fluorescence. Immunofluorescence staining of tissue sections was also conducted to evaluate the effect of Exo-MSCs$^{IL-1\beta}$ on macrophage polarization. After antigen retrieval, tissue sections were incubated with an anti-Arg-1 (1:1000, Abcam) antibody at 4°C overnight. Goat anti-rat IgG H&L (Alexa Fluor 647, Abcam) was applied for 30 min incubation at 37°C. DAPI was used to counterstain the nucleus. Finally, confocal microscopic pictures were obtained.

Transfection of THP-1 Cells with Let-7c Mimics and Inhibitors

THP-1 cells were seeded in Transwell chambers and treated with 100 ng/mL PMA for 48 h, and then transfected with a miRNA let-7c mimic, let-7c inhibitor, or negative control sequence (GenePharma, Shanghai, China) using INTERFERin transfection reagent (Polyplus Transfection, Illkirch, France) according to the manufacturer's instructions. Then they were co-cultured with the TGF-β1-induced UFBs for 48 h as indicated.

Luciferase Reporter Assay

A cDNA sequence corresponding to the human p21-activated kinase 1 (PAK1) mRNA 3′UTR and containing a sequence complementary to the seed sequence of let-7c was amplified by PCR and cloned into psiCHECK2 vector (Hedgehog Biotech, Shanghai, China) to obtain psiCHECK2-WT-PAK1. The 3′UTR was mutagenized within the let-7c-binding sequence using a QuikChange II Site-Directed Mutagenesis Kit (Agilent, Palo Alto, CA, USA) to obtain psiCHECK2-MUT-PAK1. For the luciferase assay, THP-1 cells treated with 100 ng/mL PMA were grown in 96-well plates and co-transfected with 400 ng of either psiCHECK2-WT-PAK1 or psiCHECK2-MUT-PAK1 plasmids plus 50 ng of either let-7c mimic or a negative control sequence (Invitrogen) using Lipofectamine 2000 reagent (Invitrogen). At 48 h after transfection, firefly luciferase activity was measured
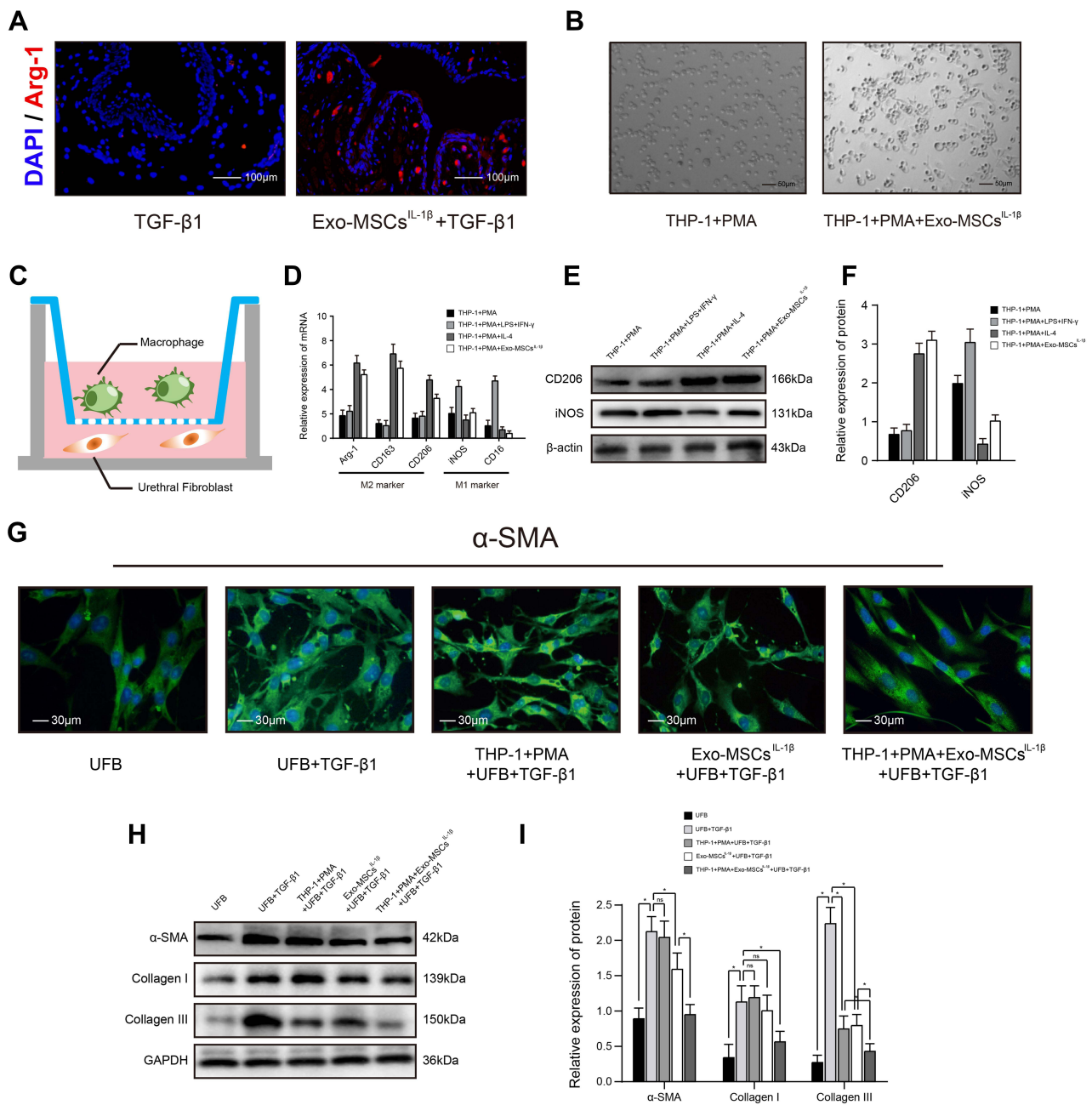
Figure 2 Exosomes from IL-1β-induced MSCs inhibit activation of urethral fibroblasts by regulating macrophage polarization in vitro. (**A**) Immunofluorescence microscopy images of Arg-1 expression in urethral tissues treated with TGF-β1 alone or TGF-β1 + Exo-MSCs[IL-1β]. (**B**) Light microscopy images showing the morphology of THP-1 cells incubated for 48 h with PMA in the presence or absence of Exo-MSCs[IL-1β]. (**C**) Schematic of the Transwell co-culture system used in this study. (**D**) qRT-PCR analysis of mRNA levels of the indicated macrophage markers in UFBs co-cultured with the indicated cells and/or factors. (**E** and **F**) Western blot analysis (**E**) and quantification of band densities (**F**) of the indicated macrophage markers in UFBs co-cultured with the indicated cells and/or factors. (**G**) Immunofluorescence microscopy images of α-SMA expression in UFBs co-cultured with the indicated cells and/or factors. (**H** and **I**) Western blot analysis (**H**) and quantification of band densities (**I**) of α-SMA, collagen I, and collagen III in UFBs co-cultured with the indicated cells and/or factors. Data in (**D, F** and **I**) are presented as the mean ± SD of at least three independent experiments and were analyzed with Student's *t*-test or one-way ANOVA (*$P < 0.05$; ns, not significant).
Abbreviations: PMA, phorbol 12-myristate 13-acetate; LPS, lipopolysaccharide; IFN-γ, interferon-γ; IL-4, interleukin-4; MSCs, mesenchymal stem cells; UFB, urethral fibroblasts; Exo-MSCs, exosomes from control MSCs; Exo-MSCs[IL-1β], exosomes from IL-1β-primed MSCs; TGF-β1, transforming growth factor-β1; IL-1β, interleukin-1β; α-SMA, α-smooth muscle actin; GAPDH, glyceraldehyde-3-phosphate dehydrogenase.

using a Dual-Luciferase assay system (Promega, Madison, WI, USA) with Renilla luciferase activity was used as internal control, according to the manufacturer's protocol.

Statistical Analysis

All analyses were performed with SPSS version 22.0 software (SPSS, Chicago, IL, USA) and GraphPad 5.0 software

(GraphPad Software, San Diego, CA, USA). *P* < 0.05 was considered statistically significant. For the bar and line graphs, data are presented as the mean ± standard deviation (SD) from at least three independent experiments. For immunoblot quantification, the gels were scanned, and the band intensities were examined with ImageJ software. For quantification of total protein, the band intensity was normalized to that of the loading control, and for quantification of phosphorylated protein, the band intensity was normalized to the corresponding total protein intensity.

Results

Exosomes from IL-1β-Induced MSCs Reduce Urethral Stricture in Rabbits

Exosomes were isolated by ultracentrifugation of supernatants from human MSCs cultured for 48 h with or without IL-1β, and the quality and purity of the exosomes was examined using a variety of methods. Transmission electron microscopy analysis revealed that the purified vesicles had the characteristic cup-shaped morphology of exosomes (Figure 1B), and nanoparticle tracking analysis showed that they had a mean ± SD diameter of 62.73 ± 38.20 nm, which is an appropriate size for exosomes (Figure 1C). Finally, WB demonstrated high expression levels of the exosomal markers TSG101 and CD63 in these vesicles, compared with those in vesicle-free supernatant (Figure 1D). Thus, the vesicles isolated from MSCs cultures were confirmed to be exosomes.

To determine the potential value of Exo-MSCs$^{IL-1\beta}$ compared with Exo-MSCs for the treatment of urethral stricture, we used a New Zealand rabbit model of posttraumatic urethral stricture in which TGF-β1 is injected directly into the urethra to induce fibrosis. After six weeks, urethrography was conducted to assess the degree of urethral stricture, and urethral scar tissue was excised for immunohistochemical staining of α-SMA, a marker of fibrosis. Notably, urethral stricture was significantly reduced in animals injected with either Exo-MSCs or Exo-MSCs$^{IL-1\beta}$ compared with animals injected with TGF-β1 alone, and Exo-MSCs$^{IL-1\beta}$ were significantly more effective than Exo-MSCs (Figure 1E and F). Consistent with this result, we observed a significant reduction in collagen fiber accumulation in urethral tissues from rabbits injected with Exo-MSCs and Exo-MSCs$^{IL-1\beta}$ compared with TGF-β1 alone, and the beneficial effect was particularly marked in the Exo-MSC$^{IL-1\beta}$ group (Figure 1G and H). These results suggest

that exosomes from IL-1β-induced MSCs can reduce urethral stricture in rabbits.

Exosomes from IL-1β-Induced MSCs Inhibit Activation of Urethral Fibroblasts by Regulating Macrophage Polarization in vitro

We examined the urethral tissues of rabbits with Exo-MSCs$^{IL-1\beta}$ treated or not and found that, the fluorescence of Arg-1 (M2 macrophage marker) was much more stronger in Exo-MSCs$^{IL-1\beta}$ group, which indicated that M2 macrophages might participate in the process (Figure 2A). Next, we examined the effects of MSC-derived exosomes on macrophage polarization by in vitro experiments. THP-1 monocytes were incubated for 48 h with the differentiation inducer PMA together with Exo-MSCs$^{IL-1\beta}$, IL-4 (M2 polarization positive control), or LPS plus IFN-γ (M1 polarization positive control). We observed a shift in the morphology of THP-1 cells towards a elongated, spindle-like shape, which is typical of the M2 macrophage subtype (Figure 2B). In addition, qRT-PCR analysis of M2 macrophage markers (Arg-1, CD163, CD206) and M1 macrophage markers (iNOS, CD16) revealed that addition of Exo-MSCs$^{IL-1\beta}$ to THP-1 cells during polarization induced a clear M2 macrophage expression profile (Figure 2D). Similar results were obtained in WB analysis (Figure 2E and F). Next, we determined whether Exo-MSCs$^{IL-1\beta}$ and/or macrophages could affect activation of UFBs by TGF-β1. To this end, we performed Transwell co-cultures in which the lower chambers contained UFBs with or without TGF-β1 activated, and the upper chambers contained medium (control); THP-1 cells + PMA; Exo-MSCs$^{IL-1\beta}$; or THP-1 cells + PMA + Exo-MSCs$^{IL-1\beta}$. After 48 h incubation, the UFBs were removed for analysis. Immunofluorescence staining of α-SMA and Western blot analysis of α-SMA, collagen I, and collagen III were performed to assess the extent of UFBs activation. We found that TGF-β1 treatment of UFBs increased the production of all three proteins, as expected. However, the combination of macrophages + Exo-MSCs$^{IL-1\beta}$ dramatically inhibited TGF-β1-induced upregulation of αSMA, collagen I, and collagen III to near-basal levels. Notably, the presence of macrophages alone or Exo-MSCs$^{IL-1\beta}$ alone had much weaker inhibitory effects than the combination (Figure 2G–I). These results suggest that macrophages and Exo-MSCs$^{IL-1\beta}$ act in concert to potently inhibit TGF-β1-induced activation of UFBs.

miRNA Let-7c is Enriched in Exosomes from IL-1β-Induced MSCs and Inhibits Myofibroblast Formation by Promoting Macrophage M2 Polarization

Increasing evidence supports an important role for miRNAs in exosome-mediated intercellular communication.[27] We therefore sought to determine whether Exo-MSCs$^{IL-1\beta}$ contained miRNAs that may contribute to the observed effects on macrophage-dependent UFB activation. qRT-PCR analysis indicated strong upregulation of let-7c expression in IL-1β-treated MSCs compared with untreated MSCs and also in Exo-MSCs$^{IL-1\beta}$ compared with Exo-MSCs (Figure 3A and B). Notably, let-7c expression in PMA-treated THP-1 cells was also increased after exposure to Exo-MSCs$^{IL-1\beta}$ but not to Exo-MSCs (Figure 3C). To determine whether the increase in let-7c levels was due to indirect induction of let-7c synthesis in macrophages or direct uptake of Exo-MSCs$^{IL-1\beta}$ into macrophages, we labeled Exo-MSCs$^{IL-1\beta}$ with the dye PKH-67 and performed fluorescence microscopy of cells after incubation with the exosomes. As shown in Figure 3D, the green fluorescence of PKH-67 is clearly concentrated in and around the cells, confirming that Exo-MSCs$^{IL-1\beta}$ were taken up into the cells. Next, we investigated the mechanism by which let-7c might affect macrophage polarization by transfecting PMA-treated THP-1 cells with a let-7c mimic, and observing the effects on polarization. We found that let-7c overexpression in THP-1 cells incubated under M1-polarizing conditions (PMA, LPS, and IFN-γ) caused a switch to the M2 macrophage subtype, as demonstrated by cell morphology (Figure 3E). Similar results were obtained in qRT-PCR analysis (Figure 3F) and WB analysis (Figure 3G and H). To examine the influence of let-7c overexpression or silencing on THP-1 polarization and subsequent activation of UFBs, THP-1 cells were transfected with a let-7c mimic or let-7c inhibitor and co-cultured with UFBs in Transwell assays as described earlier. Compared with the control UFBs (incubated with TGF-β1 + PMA + control THP-1 cells), expression of α-SMA, collagen I, and collagen III was significantly reduced in the presence of Exo-MSCs$^{IL-1\beta}$ or let-7c-overexpressing THP-1 cells (Figure 3I–K). Strikingly, incubation of UFBs with let-7c-silenced THP-1 cells had the reverse effect and markedly enhanced the expression of all three proteins in UFBs (Figure 3I–K). Thus, let-7c in Exo-MSCs$^{IL-1\beta}$ plays a key role in M2 macrophage polarization and subsequent inhibition of UFB activation.

miRNA Let-7c Promotes Macrophage M2 Polarization by Inhibiting PAK1-Dependent Activation of the NF-κB Signaling Pathway

Let-7c has been reported to inhibit activation of the NF-κB signaling pathway, which plays a key role in the polarization status of macrophages, by suppressing the function of its target PAK1, a member of serine/threonine kinase family involved in pleiotropic physiological processes including cytoskeleton dynamics and cell motility, survival, mitosis, transcription, and translation.[29,30] To determine whether this mechanism might underlie the effects of let-7c and Exo-MSCs$^{IL-1\beta}$ on M2 macrophage polarization in our experiments, we first examined the effects of a let-7c mimic and inhibitor on PAK1 expression levels in PMA-treated THP-1 cells. Indeed, PAK1 mRNA and protein levels were reduced and increased by transfection with the let-7c mimic and inhibitor, respectively (Figure 4A–C). We then employed TargetScan database to identify a putative let-7c-binding sequence in the 3′UTR of PAK1 mRNA and performed luciferase reporter assays to examine direct binding between let-7c and PAK1. Luciferase reporter plasmids were constructed containing the PAK1-3′UTR-WT or a PAK1-3′UTR-MUT carrying mutations in the predicted let-7c-binding sequence (Figure 4D). Co-transfection of PMA-treated THP-1 cells with the reporter plasmids and the let-7c mimic, but not a control sequence, markedly reduced the luciferase activity of cells transfected with the WT-PAK1 plasmid, but had no effect on the activity of cells expressing the MUT-PAK1 plasmid (Figure 4E). Thus, PAK1 mRNA is a direct target of let-7c in macrophages.

Previous studies have shown that activation of NF-κB signaling tends to polarize macrophages towards the M1 subtype, while suppression of this pathway polarizes towards the M2 subtype.[30] Therefore, we determined the effects of let-7c overexpression or silencing on the expression levels of phosphorylated (activated) components of the NF-κB pathway in macrophages. As shown in Figure 4F and G, transfection of macrophages with the let-7c inhibitor strongly induced phosphorylation of p65, IKKβ, and IκBα, while transfection with the let-7c mimic had the opposite effect, indicating that let-7c modulates activation of the NF-κB signaling pathway. Taken together, these findings suggest
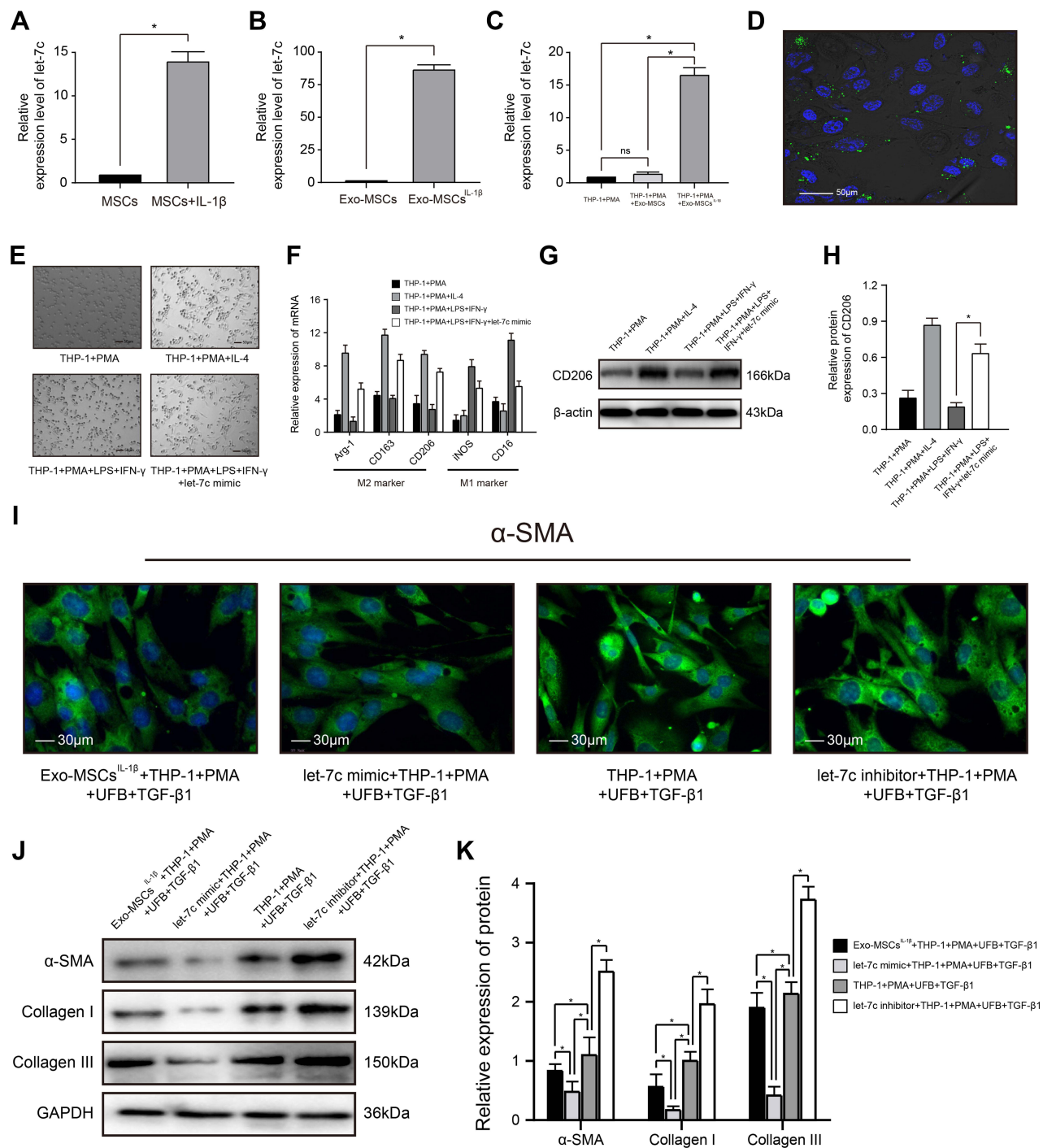
Figure 3 miRNA let-7c is enriched in exosomes isolated from IL-1β-induced MSCs and inhibits myofibroblast formation by promoting macrophage M2 polarization. (**A–C**) qRT-PCR analysis of let-7c expression in (**A**) MSCs incubated with or without IL-1β for XX h; (**B**) Exo-MSCs or Exo-MSCs$^{IL-1β}$; and (**C**) THP-1 cells treated with saline + PMA, Exo-MSCs + PMA, or Exo-MSCs$^{IL-1β}$ + PMA for 48 h. (**D**) Epifluorescence images of uptake of PKH-67-labeled exosomes (green) taken up by PMA-treated THP-1 cells. Nuclei were stained with Hoechst 33342 (blue). (**E**) Light microscopy images showing THP-1 cells incubated with the indicated factors. (**F**) qRT-PCR analysis of mRNA expression levels of the indicated macrophage markers after incubation of THP-1 cells with the indicated factors. (**G** and **H**) Western blot analysis (**G**) and quantification of band densities (**H**) of CD206 after incubation of THP-1 cells with the indicated factors. (**I**) Immunofluorescence images of α-SMA expression in UFBs after incubation with the indicated cells and factors. (**J** and **K**) Western blot analysis (**J**) and quantification of band densities (**K**) of α-SMA, collagen I, and collagen III in UFBs treated as described for (**I**). Data in (**A–C, F, H**, and **K**) are presented as the mean ± SD of at least three independent experiments and were analyzed with Student's *t*-test or one-way ANOVA (*$P < 0.05$).
Abbreviations: PMA, phorbol 12-myristate 13-acetate; LPS, lipopolysaccharide; IFN-γ, interferon-γ; IL-4, interleukin-4; MSCs, mesenchymal stem cells; UFB, urethral fibroblasts; Exo-MSCs, exosomes from control MSCs; Exo-MSCs$^{IL-1β}$, exosomes from IL-1β-primed MSCs; TGF-β1, transforming growth factor-β1; IL-1β, interleukin-1β; α-SMA, α-smooth muscle actin; GAPDH, glyceraldehyde-3-phosphate dehydrogenase.
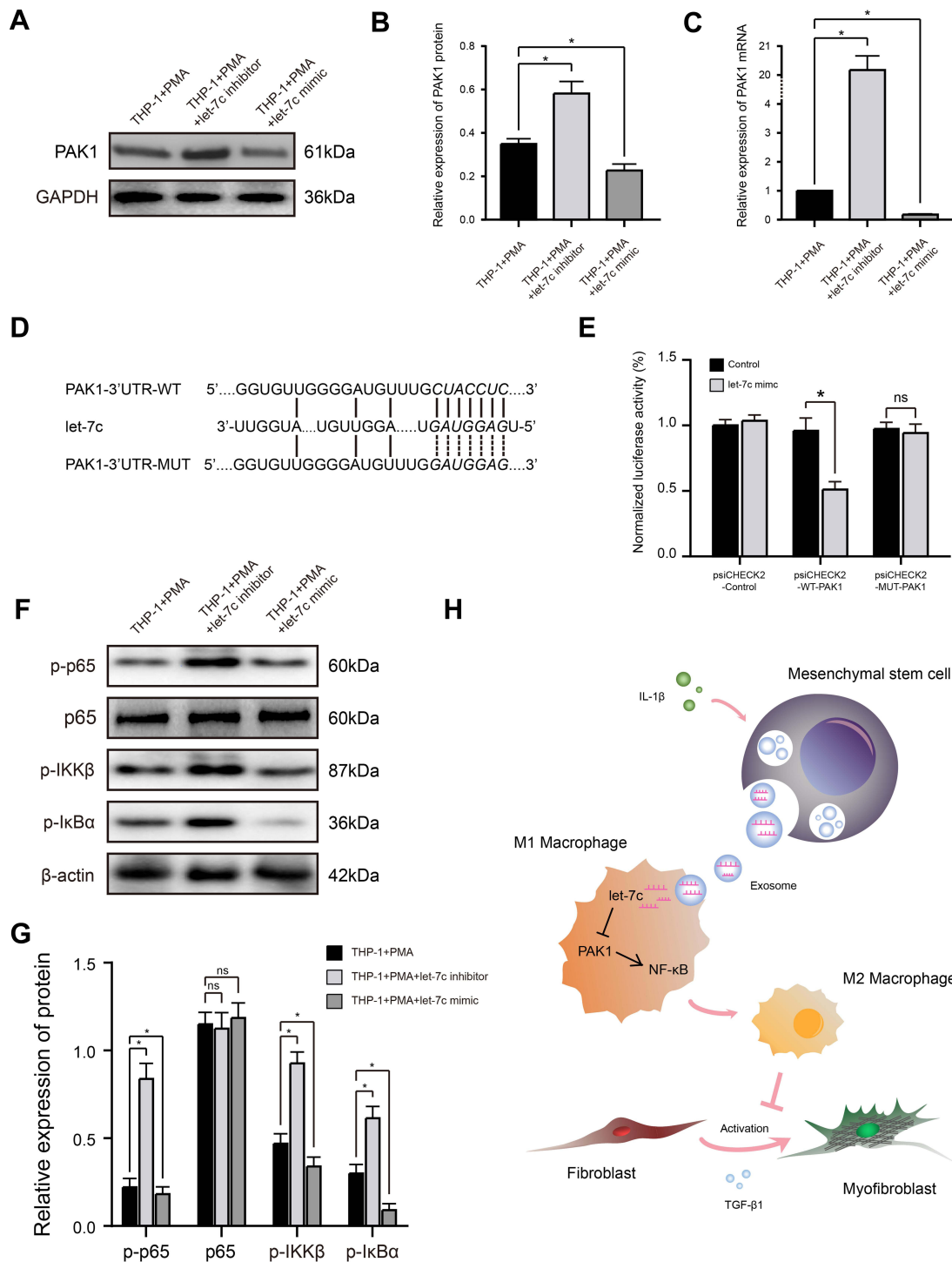
Figure 4 miRNA let-7c promotes macrophage M2 polarization by inhibiting the PAK1-dependent NF-κB signaling pathway. (**A** and **B**) Western blot analysis (**A**) and quantification of band densities (**B**) of PAK1 expression in PMA-treated THP-1 cells transfected with control, let-7c inhibitor, or let-7c mimic. (**C**) qRT-PCR analysis of PAK1 mRNA expression level in PMA-treated THP-1 cells transfected as described in (**A**). (**D**) Putative let-7c-binding sites in the PAK1-3′UTR-WT sequence, and the location of mutated residues in PAK1-3′UTR-MUT. (**E**) Relative luciferase activity in THP-1 cells co-transfected with a let-7c mimic and either empty vector, PAK1-3′UTR-WT, or PAK1-3′UTR-MUT vectors. (**F** and **G**) Western blot analysis (**F**) and quantification of band densities (**G**) of the indicated phosphorylated (p) markers of the NF-κB signaling pathway in PMA-treated THP-1 cells transfected as described for (**A**). (**H**) Proposed model based on the results of this study. Data in (**B, C, E,** and **G**) are presented as the mean ± SD of at least three independent experiments and were analyzed with Student's *t*-test or one-way ANOVA (*$P < 0.05$; ns, not significant).
Abbreviations: PAK1, p21-activated kinase 1; GAPDH, glyceraldehyde-3-phosphate dehydrogenase; WT, wild type; MUT, mutant type; IL-1β, interleukin-1β; TGF-β1, transforming growth factor-β1.

that Exo-MSCs$^{IL-1\beta}$ promote macrophage M2 polarization by let-7c-mediated inhibition of PAK1-dependent NF-κB signaling (Figure 4H).

Discussion

In this study, we have shown that exosomes derived from IL-1β-induced MSCs contain let-7c and promote M2 macrophage polarization in vitro. Moreover, let-7c-containing Exo-MSCs$^{IL-1\beta}$ not only inhibit M2 macrophage-dependent activation of UFBs in vitro but are also beneficial in a rabbit model of urethral stricture. We also demonstrated that let-7c promotes M2 macrophage polarization via inhibition of PAK1-dependent NF-κB signaling pathway, which, in turn, inhibits UFB differentiation into myofibroblasts and reduce fibrosis. These results therefore demonstrate that let-7c plays a crucial role in the development of urethral fibrosis and may represent a promising therapeutic target for this condition. To the best of our knowledge, this is the first report that IL-1β treatment of MSCs increases let-7c expression and improves urethral stricture by regulating macrophage M2 polarization.

Scar formation within the urethral lumen after trauma is a major cause of urethral stricture, which is difficult to treat and readily relapses.[31] Macrophages have well-established roles as key mediators of the physiological process of wound healing as well as in pathological conditions such as liver, renal, and myocardial fibrosis and systemic sclerosis.[32–34] M2 macrophages can protect against myocardial remodeling after ischemia–reperfusion injury by regulating activation of the platelet-derived growth factor receptor kinase in cardiac fibroblasts.[35] Hou et al reported that sonic hedgehog secreted by fibrosis-associated alveolar epithelial cells can promote the development of pulmonary fibrosis via osteopontin-mediated alternative activation of macrophages.[36] Similarly, our study demonstrated that M2 macrophages play a crucial role in the post-traumatic urethral healing process. Our in vitro experiments suggested that Exo-MSCs$^{IL-1\beta}$ alone could not inhibit UFB activation; instead, macrophages were necessary to reduce α-SMA, collagen I, and collagen III expression, indicating that macrophages acted as an intermediate bridge between MSCs and UFBs. We concluded that Exo-MSC$^{IL-1\beta}$-polarized M2 macrophages secreted factors that were able to diffuse through the semipermeable membranes of Transwell chambers to activate UFBs.

Our recent study revealed that MSCs can directly suppress TGF-β1-induced myofibroblast formation and the release of pro-inflammatory factors during post-traumatic urethral healing, which is a well-known effect of MSCs on fibroblasts.[15] However, whether MSCs could act indirectly on UFBs was unknown. MSCs are known to have various immunosuppressive and anti-inflammatory effects. MSCs can not only induce the production of anti-inflammatory immune cells through ligand–receptor interactions or miRNA-mediated mechanisms, but they can also regulate the secretion of anti-inflammatory cytokines by immune cells.[21] Thus, we considered the possibility that MSCs may indirectly regulate fibroblast activation through immune cells; specifically, by regulating the phenotype of macrophages. Indeed, we demonstrated that exosomes from IL-1β-treated MSCs could promote M2 macrophage polarization and subsequently prevent TGF-β1-induced UFB activation, which was consistent with our hypothesis.

Let-7c is an anti-inflammatory miRNA and plays important roles in immune regulation.[37–39] In patients with rheumatoid arthritis, high expression level of let-7c led to decreased levels of TNF-α, IL-2, and IL-6, suggesting suppression of the inflammatory response.[40] Let-7c can also regulate inflammation under oxidative stress in lens epithelial cells by targeting ATG3, which prevents the formation of cataracts.[41] In the present study, we found that let-7c was a key signaling factor for macrophage polarization and inhibition of UFB activation. We also showed that let-7c expression negatively regulates PAK1 expression and NF-κB pathway activation, which is consistent with the results reported by Zhang et al.[29]

In conclusion, this study demonstrates that exosomes derived from IL-1β-primed MSCs can regulate the polarization of macrophages and activation of UFBs, thereby significantly reducing urethral tissue fibrosis and urethral stricture. Our findings identify the let-7c/PAK1/NF-κB axis as a promising therapeutic target for patients with urethral stricture.

Ethical Approval and Informed Consent

experiments were approved by the Experimental Animal Ethics Committee of Fujian Medical University.

Disclosure

All authors declared that there were no conflicts of interest.

References

1. Santucci RA, Joyce GF, Wise M. Male urethral stricture disease. *J Urol*. 2007;177(5):1667–1674. doi:10.1016/j.juro.2007.01.041
2. Li XD, Wu YP, Chen SH, et al. Fasudil inhibits actin polymerization and collagen synthesis and induces apoptosis in human urethral scar fibroblasts via the Rho/ROCK pathway. *Drug Des Devel Ther*. 2018;12:2707–2713. doi:10.2147/dddt.s156095.
3. Xu N, Chen SH, Qu GY, et al. Fasudil inhibits proliferation and collagen synthesis and induces apoptosis of human fibroblasts derived from urethral scar via the Rho/ROCK signaling pathway. *Am J Transl Res*. 2017;9(3):1317–1325.
4. Lumen N, Hoebeke P, Willemsen P, et al. Etiology of urethral stricture disease in the 21st century. *J Urol*. 2009;182(3):983–987. doi:10.1016/j.juro.2009.05.023
5. Ribeiro-Filho LA, Sievert KD. Acellular matrix in urethral reconstruction. *Adv Drug Deliv Rev*. 2015;82-83:38–46. doi:10.1016/j.addr.2014.11.019
6. Hampson LA, McAninch JW, Breyer BN. Male urethral strictures and their management. *Nat Rev Urol*. 2014;11(1):43–50. doi:10.1038/nrurol.2013.275
7. Shaw NM, Venkatesan K. Endoscopic management of urethral stricture: review and practice algorithm for management of male urethral stricture disease. *Curr Urol Rep*. 2018;19(3):19. doi:10.1007/s11934-018-0771-6
8. Tian Y, Wazir R, Yue X, et al. Prevention of stricture recurrence following urethral endoscopic management: what do we have? *J Endourol*. 2014;28(5):502–508. doi:10.1089/end.2013.0538
9. Park JJ, Kuo TL, Chapple CR. Mitomycin C in the treatment of anterior urethral strictures. *Nat Rev Urol*. 2018;15(12):717–718. doi:10.1038/s41585-018-0102-1
10. Andersen HL, Duch BU, Gregersen H, et al. The effect of the somatostatin analogue lanreotide on the prevention of urethral strictures in a rabbit model. *Urol Res*. 2003;31(1):25–31. doi:10.1007/s00240-003-0296-3
11. Kurt O, Gevher F, Yazici CM, et al. Effect of mitomycin - C and triamcinolone on preventing urethral strictures. *Int Braz J Urol*. 2017;43(5):939–945. doi:10.1590/s1677-5538.ibju.2016.0191
12. Krane LS, Gorbachinsky I, Sirintrapun J, et al. Halofuginone-coated urethral catheters prevent periurethral spongiofibrosis in a rat model of urethral injury. *J Endourol*. 2011;25(1):107–112. doi:10.1089/end.2010.0514
13. Hofer MD, Cheng EY, Bury MI, et al. Analysis of primary urethral wound healing in the rat. *Urology*. 2014;84(1):246.e241–247. doi:10.1016/j.urology.2014.04.012

14. Krzyszczyk P, Schloss R, Palmer A, et al. The role of macrophages in acute and chronic wound healing and interventions to promote pro-wound healing phenotypes. *Front Physiol*. 2018;9:9419. doi:10.3389/fphys.2018.00419
15. Liang YC, Wu YP, Li XD, et al. TNF-α-induced exosomal miR-146a mediates mesenchymal stem cell-dependent suppression of urethral stricture. *J Cell Physiol*. 2019;234(12):23243–23255. doi:10.1002/jcp.28891
16. Essandoh K, Li Y, Huo J, et al. MiRNA-mediated macrophage polarization and its potential role in the regulation of inflammatory response. *Shock*. 2016;46(2):122–131. doi:10.1097/SHK.0000000000000604
17. Mescher AL. Macrophages and fibroblasts during inflammation and tissue repair in models of organ regeneration. *Regeneration (Oxf)*. 2017;4(2):39–53. doi:10.1002/reg2.77
18. Lucas T, Waisman A, Ranjan R, et al. Differential roles of macrophages in diverse phases of skin repair. *J Immunol*. 2010;184(7):3964–3977. doi:10.4049/jimmunol.0903356
19. Hesketh M, Sahin KB, West ZE, et al. Macrophage phenotypes regulate scar formation and chronic wound healing. *Int J Mol Sci*. 2017;18(7):1545. doi:10.3390/ijms18071545
20. Ueshima E, Fujimori M, Kodama H, et al. Macrophage-secreted TGF-β 1 contributes to fibroblast activation and ureteral stricture after ablation injury. *Am J Physiol Renal Physiol*. 2019;317(1):F52–f64. doi:10.1152/ajprenal.00260.2018
21. Qian X, An N, Ren Y, et al. Immunosuppressive effects of mesenchymal stem cells-derived exosomes. *Stem Cell Rev Rep*. 2021;17(2):411-427. doi:10.1007/s12015-020-10040-7
22. Deng H, Wu L, Liu M, et al. Bone marrow mesenchymal stem cell-derived exosomes attenuate LPS-induced ARDS by modulating macrophage polarization through inhibiting glycolysis in macrophages. *Shock*. 2020;54(6):828–843. doi:10.1097/SHK.0000000000001549
23. Zhao J, Li X, Hu J, et al. Mesenchymal stromal cell-derived exosomes attenuate myocardial ischaemia-reperfusion injury through miR-182-regulated macrophage polarization. *Cardiovasc Res*. 2019;115(7):1205–1216. doi:10.1093/cvr/cvz040
24. Liu J, Qiu X, Lv Y, et al. Apoptotic bodies derived from mesenchymal stem cells promote cutaneous wound healing via regulating the functions of macrophages. *Stem Cell Res Ther*. 2020;11(1):507. doi:10.1186/s13287-020-02014-w
25. Broekman W, Amatngalim GD, de Mooij-eijk Y, et al. TNF-α and IL-1β-activated human mesenchymal stromal cells increase airway epithelial wound healing in vitro via activation of the epidermal growth factor receptor. *Respir Res*. 2016;17:173. doi:10.1186/s12931-015-0316-1
26. Song Y, Dou H, Li X, et al. Exosomal miR-146a contributes to the enhanced therapeutic efficacy of interleukin-1β-primed mesenchymal stem cells against sepsis. *Stem Cells*. 2017;35(5):1208–1221. doi:10.1002/stem.2564
27. Alexander M, Hu R, Runtsch MC, et al. Exosome-delivered microRNAs modulate the inflammatory response to endotoxin. *Nat Commun*. 2015;6:67321. doi:10.1038/ncomms8321
28. Wu YP, Ke ZB, Zheng WC, et al. Kinesin family member 18B regulates the proliferation and invasion of human prostate cancer cells. *Cell Death Dis*. 2021;12(4):302. doi:10.1038/s41419-021-03582-2
29. Zhang W, Liu H, Liu W, et al. Polycomb-mediated loss of microRNA let-7c determines inflammatory macrophage polarization via PAK1-dependent NF-κB pathway. *Cell Death Differ*. 2015;22(2):287–297. doi:10.1038/cdd.2014.142
30. Banerjee S, Xie N, Cui H, et al. MicroRNA let-7c regulates macrophage polarization. *J Immunol*. 2013;190(12):6542–6549. doi:10.4049/jimmunol.1202496
31. Castiglione F, Dewulf K, Hakim L, et al. Adipose-derived stem cells counteract urethral stricture formation in rats. *Eur Urol*. 2016;70(6):1032–1041. doi:10.1016/j.eururo.2016.04.022

32. Chistiakov DA, Orekhov AN, Bobryshev YV. The role of cardiac fibroblasts in post-myocardial heart tissue repair. *Exp Mol Pathol*. 2016;101(2):231–240. doi:10.1016/j.yexmp.2016.09.002

33. Ma PF, Gao CC, Yi J, et al. Cytotherapy with M1-polarized macrophages ameliorates liver fibrosis by modulating immune microenvironment in mice. *J Hepatol*. 2017;67(4):770–779. doi:10.1016/j.jhep.2017.05.022

34. Chen L, Sha ML, Li D, et al. Relaxin abrogates renal interstitial fibrosis by regulating macrophage polarization via inhibition of Toll-like receptor 4 signaling. *Oncotarget*. 2017;8(13):21044–21053. doi:10.18632/oncotarget.15483

35. Yue Y, Huang S, Li H, et al. M2b macrophages protect against myocardial remodeling after ischemia/reperfusion injury by regulating kinase activation of platelet-derived growth factor receptor of cardiac fibroblast. *Ann Transl Med*. 2020;8(21):1409. doi:10.21037/atm-20-2788

36. Hou J, Ji J, Chen X, et al. Alveolar epithelial cell-derived Sonic hedgehog promotes pulmonary fibrosis through OPN-dependent alternative macrophage activation. *Febs J*. 2021;288(11):3530-3546. doi:10.1111/febs.15669

37. Jaiswal A, Maurya M, Maurya P, et al. Lin28B regulates angiotensin II-mediated let-7c/miR-99a microRNA formation consequently affecting macrophage polarization and allergic inflammation. *Inflammation*. 2020;43(5):1846–1861. doi:10.1007/s10753-020-01258-1

38. Yuan H, Zhao H, Wang J, et al. MicroRNA let-7c-5p promotes osteogenic differentiation of dental pulp stem cells by inhibiting lipopolysaccharide-induced inflammation via HMGA2/PI3K/Akt signal blockade. *Clin Exp Pharmacol Physiol*. 2019;46(4):389–397. doi:10.1111/1440-1681.13059

39. Yuan H, Zhang H, Hong L, et al. MicroRNA let-7c-5p suppressed lipopolysaccharide-induced dental pulp inflammation by inhibiting dentin matrix protein-1-mediated nuclear factor kappa B (NF-κB) pathway in vitro and in vivo. *Med Sci Monit*. 2018;24:6656–6665. doi:10.12659/MSM.909093

40. Wang ZQ, Xiu DH, Jiang JL, et al. Long non-coding RNA XIST binding to let-7c-5p contributes to rheumatoid arthritis through its effects on proliferation and differentiation of osteoblasts via regulation of STAT3. *J Clin Lab Anal*. 2020;34(11):e23496. doi:10.1002/jcla.23496

41. Li T, Huang Y, Zhou W, et al. Let-7c-3p regulates autophagy under oxidative stress by targeting ATG3 in lens epithelial cells. *Biomed Res Int*. 2020;20206069390. doi:10.1155/2020/6069390